

Thermal shock parameters [R , R''' and R''''] of magnesia–spinel composites

Cemail Aksel^{*,1}, Paul D. Warren²

Department of Materials, School of Process, Environmental and Materials Engineering, University of Leeds, Leeds LS2 9JT, UK

Received 20 September 2001; received in revised form 20 May 2002; accepted 25 May 2002

Abstract

Thermal shock parameters (R , R''' and R'''') have been calculated using measured strength and modulus values for model magnesia–spinel composite materials. The R''' and R'''' parameters vary with both spinel content (0–30%) and spinel particle size (3–22 μm). In general, the larger the spinel content, the higher the values of R''' and R'''' . It is predicted that the coarsest (22 μm) spinel provides a significant improvement in resistance to thermal shock damage through maximised difficulty of crack propagation, with a maximum at $\sim 20\%$ addition. These predictions were also matched by thermal shock testing. After quenching from 1000 $^{\circ}\text{C}$, the 20% 22 μm spinel composite had a retained strength ~ 4.5 times higher than that for similarly quenched pure magnesia.

© 2002 Elsevier Science Ltd. All rights reserved.

Keywords: Composites; Mechanical properties; MgAl_2O_4 ; MgO ; Microcracking; Thermal shock damage resistance (R''' and R'''') parameters; Thermal stress resistance (R) parameter

1. Introduction

A traditional standardised method used to characterise the thermal shock resistance of ceramic materials involves quenching samples from high temperatures by using water, oil or air as a cooling medium. A variety of post-quench responses is possible. If the material is initially strong and the temperature drop is not large, there will be a small loss in strength; if the material is initially strong and the temperature drop is large, there will be a catastrophic loss in strength. This is the typical response of engineering ceramics. For typical refractory materials, the initial strength may be low — but the strength after quenching shows little drop. Obviously, quench tests can be repeated and in this case the number of cycles necessary to cause a defined damage or weight loss can be used as a measure of thermal shock resistance.¹ On the basis of these tests, two types of parameters have been used² to predict the thermal shock behaviour of magnesia (MgO) and spinel (MgAl_2O_4) composites:

(i) thermal stress resistance, and (ii) thermal shock damage. The first determines the minimum thermal shock required to initiate a crack, and resistance to *initiation* of fracture by thermal stresses. The second expresses the degree of possibility for *further* damage caused by thermal shock.

1.1. Thermal stress resistance parameters

The appropriate parameter for a material initially damaged or undamaged, which expresses the tendency for cracks to be developed, and therefore loss in strength, can be considered to be that for the initiation of fracture caused by thermal stresses. This has been expressed^{3–7} by using an infinite slab symmetrically heated or cooled with a constant heat transfer coefficient to derive thermal shock fracture resistance parameters R , R' and R'' using the equations:

$$R = \frac{\sigma_f (1 - \nu)}{E\alpha}; \quad (1)$$

$$R' = \frac{\sigma_f (1 - \nu)k}{E\alpha} \quad (2)$$

$$\text{and } R'' = \frac{\sigma_f (1 - \nu)\phi}{E\alpha} \quad (3)$$

* Corresponding author.

E-mail address: caksel@anadolu.edu.tr (C. Aksel).

¹ Now at: Department of Materials Science and Engineering, Anadolu University, İki Eylül Campus, Muttalip, 26555 Eskişehir, Turkey.

² Now at: Pilkington plc., Group Research, Technology Centre, Hall Lane, Lathom, Lancs L40 5UF, UK.

where σ_f is the bend strength, E is Young's modulus, α the mean thermal expansion coefficient, ν Poisson's ratio, k thermal conductivity, and ϕ a stress reduction term.

The use of these parameters depends on the exact details of the temperature gradients in the material, controlled by the Biot modulus, $\beta = ah/k$, where a is the radius or half-width of the specimen and h is the heat-transfer coefficient between the body and the quenching specimen. The parameter R is applicable for the case of an instantaneous change in surface temperature for conditions of rapid heat transfer; R' is for a relatively low Biot modulus ($\beta < 2$) for conditions of slow heat transfer, R'' is for a constant heating or cooling rate.⁷ The stress reduction term ϕ is a function of the Biot Modulus. R defines the minimum temperature difference to produce fracture under conditions of infinite heat-transfer coefficient, i.e. $\phi = 1$. Looking at the parameters R , R' and R'' it is clear that high resistance to fracture initiation can be achieved in materials with high strength and thermal conductivity, and with low values of thermal expansivity and Young's modulus. However, avoiding thermal fracture by increasing strength in order to make initiation difficult is dangerous because once initiated, the high level of attained elastic strain energy means that crack propagation will be fast and catastrophic.

It should be noted that the above equations take no account of the variations of the material parameters with temperature. The coefficient of thermal expansion normally increases with increasing temperature; however, thermal conductivity decreases.

1.2. Thermal shock damage resistance parameters

Hasselmann approached the problem of thermal shock damage by considering the conditions for relative comparison of the 'degree of damage' on the basis of crack propagation, rather than those for fracture initiation. Once cracking is initiated, the maximum surface area (S_{\max}) of the fracture face is limited by $S_{\max} \leq U/\gamma_{\text{WOF}}$, where U is the elastic stored energy per unit volume and γ_{WOF} is the effective surface energy or work of fracture per unit projected area of fracture face. It is suggested that¹ a thermal shock damage or toughness parameter involving U/γ_{WOF} should be useful for comparing amounts of cracking. (The work of fracture, γ_{WOF} , represents the energy to propagate a crack over a large area, rather than that to initiate fracture.⁸ γ_{WOF} is usually interpreted as the work done in propagating a crack to break a notched specimen, divided by twice the fracture surface area, since two new faces are created.)

Hasselmann derived the following thermal shock damage resistance parameters R''' and R'''' , expressing the ability of the material to resist crack propagation

and further damage and loss of strength on thermal shocking:^{2,5,9}

$$R''' = \frac{E}{\sigma_f^2} \cdot \frac{1}{(1-\nu)} \quad (4)$$

$$\text{and } R'''' = \frac{E}{\sigma_f^2} \cdot \frac{\gamma_{\text{WOF}}}{(1-\nu)} \quad (5)$$

The R''' parameter gives information about the minimum in the elastic energy at fracture available for crack propagation, high values of the modulus indicating an improvement in thermal shock resistance. The R'''' parameter is the minimum in the extent of crack propagation on initiation of thermal stress fracture. The parameter R'''' can be used to compare the degree of damage of materials with widely different values of γ_{WOF} , such as brittle and ductile materials. R''' can also be used to compare the relative degree of damage to materials with similar crack propagation properties, i.e. the same values of γ_{WOF} .¹⁰

The criteria for minimising the extent of crack propagation, and for obtaining a low degree of damage,² are high values of the Young's modulus, Poisson's ratio, and surface energy, and low strength. Although high values of the thermal shock damage resistance parameters R''' and R'''' are desirable, it is clear that these parameters can not be maximised by letting the strength (σ_f) approach zero. There must be some intermediate value of strength and a resulting degree of damage such that the strength (after thermal shock) remains acceptable.

1.3. Applications to refractory materials

Refractories are not very resistant to the initiation of fracture from thermal stresses, but may have a significant resistance to crack propagation or extension caused by thermal shock.¹¹ Therefore, predictions made from the calculated R''' and R'''' parameters should be taken into account in characterising thermal shock damage and the retained strength of materials, rather than the thermal stress resistance parameters, i.e. R , R' and R'' .

The addition of spinel into MgO–spinel refractories leads to a noticeable improvement of thermal shock resistance, compared to MgO refractories. Retained strength and Young's modulus of both MgO and MgO–spinel materials have been reported as a function of number of quenching cycles.¹² Both retained strength and Young's modulus of MgO decrease significantly with increasing number of quenching cycles; however, those values for MgO–spinel refractories remain almost at the same level with increasing number of quenching cycles. The reason for the improved thermal shock resistance¹³ has been linked to the large difference in thermal expansion coefficient between MgO ($\sim 13.5 \text{ MK}^{-1}$) and spinel

($\sim 7.6 \text{ MK}^{-1}$).^{14,15} On cooling from the fabrication temperature in the region of 1700 °C it is believed that the thermal expansion mismatch leads to large tensile hoop stresses and microcrack development around the spinel grains. The fracture mechanism in MgO–spinel refractories relies on the development of microcracks, in which fracture occurs in a quasi-static manner, and crack branching makes propagation more difficult.^{13,16}

In this work, the effects of spinel particles (as a function of both size and volume fraction) in high purity, fully dense and relatively fine grain MgO on the Hasselman thermal shock parameters (R , R''' , and R'''') are predicted from determination of the relevant thermo-mechanical parameters. The predicted thermal shock parameters are then compared with actual thermal shock behaviour. The intention of this work was to confirm the reliability of thermal shock parameters and establish the influences of both spinel particle size and level of addition of these model finer grain composite materials. It is considered that this paper will provide a platform for extended work on less pure materials, and for predicting the detailed modelling of the thermal shock behaviour and high temperature properties of materials with compositions and microstructures matching those of commercial refractory materials.

2. Experimental

MgO of >98.0% purity ('light': GPR, BDH, Poole, UK), a nano-particle size powder, was calcined at 1300 °C for 2 h to produce a powder with a mean particle size of 0.5 μm . Alcoa MR66 spinel powder (99.5% purity) was air classified to obtain more narrow distributions of median sizes 3, 11 and 22 μm . MgO discs 30 mm in diameter were hot-pressed in graphite dies at 1700 °C and 20 MPa for 25 min, to yield material of >97% density. The MgO–spinel composites, prepared using 5 to 30 wt.% spinel, could be obtained theoretically dense ($\sim 99\%$), by hot-pressing at 1720 °C and 20 MPa for 25 min. Bulk density and apparent porosity were measured using the standard water immersion method.¹⁷ To obtain suitable samples for mechanical property measurements, disc surfaces were ground with progressively finer SiC grits down to 1000 mesh, and the tensile faces were finally diamond polished to 1 μm . Discs were then cut into bars $\sim 26 \times 3 \times 3 \text{ mm}^3$ for strength measurements. Mechanical measurements of all the spinel composites have been carried out in three-point bend, where the support roller span was 20 mm, and the cross-head speed was 0.2 mm min^{-1} . The standard equations for the strength¹⁸ (σ) and Young's Modulus¹⁹ (E) of a bar in three-point bend are:

$$\sigma = \frac{3PL}{2WD^2} \quad (6)$$

$$E = \frac{L^3m}{4WD^3} \quad (7)$$

where P =load at fracture, L =outer (support) span, W =specimen width, D =specimen thickness, and m =slope of the tangent of the initial straight-line portion of the load-deflection curve corrected for machine stiffness. Five specimens were normally tested to obtain a mean value, using a tensile testing machine (Mayes, SMT50). γ_{WOF} was calculated from load-deflection curves obtained from notched bars (c is the notch depth) deformed in three-point bend, by measuring the area (A) under the load-deflection curve, as given by the following equation:²⁰

$$\gamma_{\text{WOF}} = \frac{A}{2W(D-c)} \quad (8)$$

Thermal shock parameters R and R''' were calculated using the strength and mechanical modulus values. Thermal expansion coefficients of composites, depending on the Young's modulus, volume fraction and coefficient of thermal expansion of each component, were calculated for a two-component system with the equation derived by Turner.²¹ The R'''' parameter was calculated from R''' using the experimental values of γ_{WOF} , determined from the areas under the load-deflection curve.

Thermal-shock tests were made by holding the rectangular specimens for at least 20 min to allow for temperature equilibration in a vertical tube furnace maintained at 1000 °C and dropping them into a container of silicon oil at room temperature, which was being stirred with a magnetic stirrer (at room temperature). After cleaning with acetone, samples were dried in an oven at 110 °C before breaking in three-point bend. The strengths of the quenched samples were measured, and retained strengths of both MgO and composites were determined. Thermal shock results were then evaluated on the basis of the calculated R''' and R'''' parameters.

The CamScan 4 SEM used in this study was equipped with an EDAX system for element analysis. Secondary electron images (SEI) were used to examine the size and shape of the grains in the fracture surface of both MgO and composites; back scattered electron images (BEI), which provide atomic contrast, were used to indicate the presence and position of spinel particles in the polished surface of the composite materials.

3. Results and discussion

Because of the importance of the strength and Young's modulus (σ/E or E/σ^2) ratios for calculation of thermal shock parameters (R , R''' , and R''''), it was of interest to investigate how strength and Young's modulus

varied for each composition. Strength and Young's moduli of composites, containing spinel, decreased with increasing spinel content, for all particle sizes (Table 1). The influence of the spinel was greater, the larger the particle size.

Fig. 1 shows that there was not such a marked fall off in Young's modulus values with increasing spinel content, compared to strength. The strength was more sensitive to spinel content than was Young's modulus. The 22 μm spinel composite showed a marked decrease (by a factor of ~ 3.5) in Young's modulus with increasing spinel additions, whereas the corresponding strength values declined by a factor of ~ 4 over the same range.

3.1. *R* parameter

The *R* parameter initially decreased very slightly with spinel content, for 3 and 11 μm spinel composites, and reached a minimum at about 10% addition; further additions of spinel resulted in slight increases in the *R* parameter (Fig. 2). The *R* parameter for 22 μm spinel composites decreased with additions of up to $\sim 20\%$, and then increased with further additions of spinel to the value for pure MgO, within experimental error. The reason for the marked decline in the *R* parameter is that thermal expansion mismatch between MgO and spinel led to extensive pre-existing connecting microcracking in composite materials (Figs. 3 and 4). The 22 μm spinel composites showed the greatest sensitivity to spinel content, and would be expected on the basis of the *R* parameter to show less resistance to fracture initiation by the thermal stresses than those of finer spinel composites (Fig. 2). This indicates that strength is more sensitive to composition than is Young's modulus (Table 1 and Fig. 1). It appears that both strength and Young's modulus are controlled by the extent of microcracking with strength being influenced more strongly, until very high spinel contents are reached (Figs. 3 and 4). It would not be expected on this basis that spinel additions would improve the thermal shock resistance of MgO, through improvement of resistance to fracture initiation by the thermal stresses. It would be

Table 1

Strength and Young's modulus of MgO–spinel composites as a function of spinel content and particle size

Spinel content (wt.%)	Particle size/ μm					
	3	11	22	3	11	22
	Strength (MPa)			Young's modulus (GPa)		
0	233 \pm 7	233 \pm 7	233 \pm 7	268 \pm 30	268 \pm 30	268 \pm 30
5	206 \pm 14	163 \pm 7	158 \pm 10	247 \pm 23	229 \pm 15	215 \pm 42
10	149 \pm 22	129 \pm 45	110 \pm 24	211 \pm 52	182 \pm 42	152 \pm 38
20	124 \pm 31	111 \pm 3	65 \pm 8	168 \pm 49	147 \pm 9	111 \pm 20
30	111 \pm 47	76 \pm 11	61 \pm 4	146 \pm 54	93 \pm 14	80 \pm 5

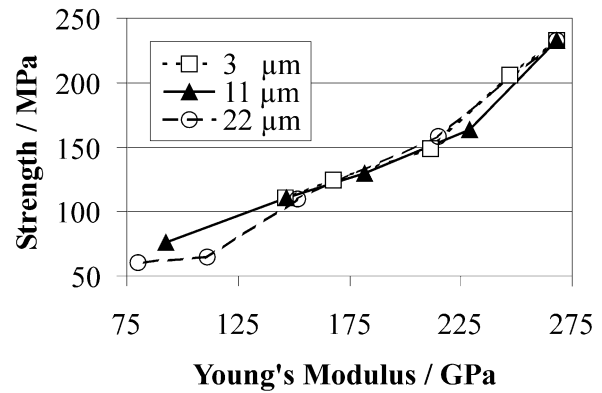


Fig. 1. Strength as a function of Young's modulus for different spinel particle size and composition of MgO–spinel composites.

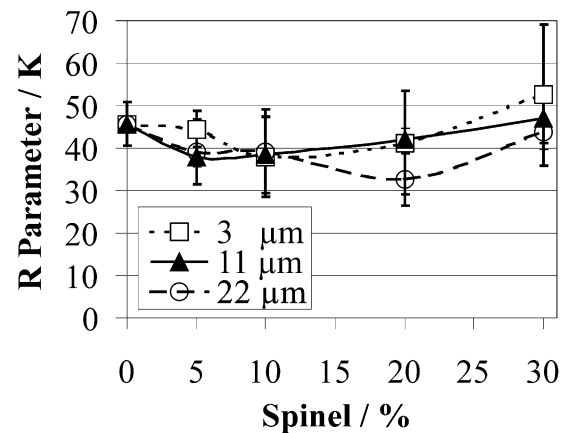


Fig. 2. *R* parameter as a function of spinel content and particle size.

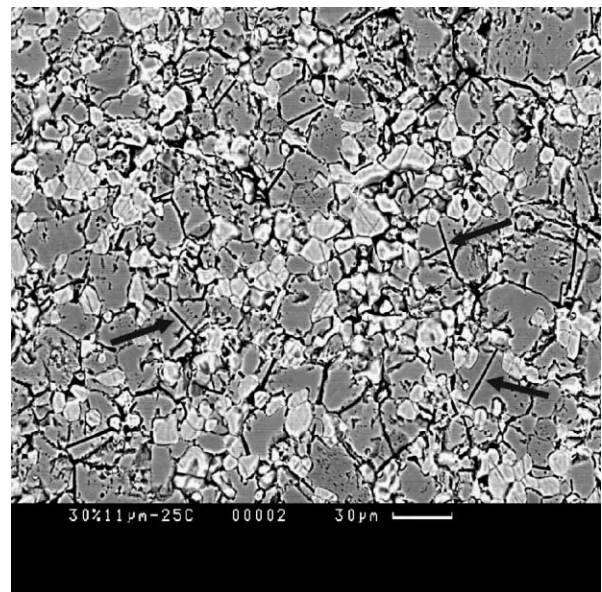


Fig. 3. SEM micrographs of thermally etched polished surfaces of 30% 11 μm spinel composite materials, showing microcracking (dark gray: MgO, light gray: spinel).

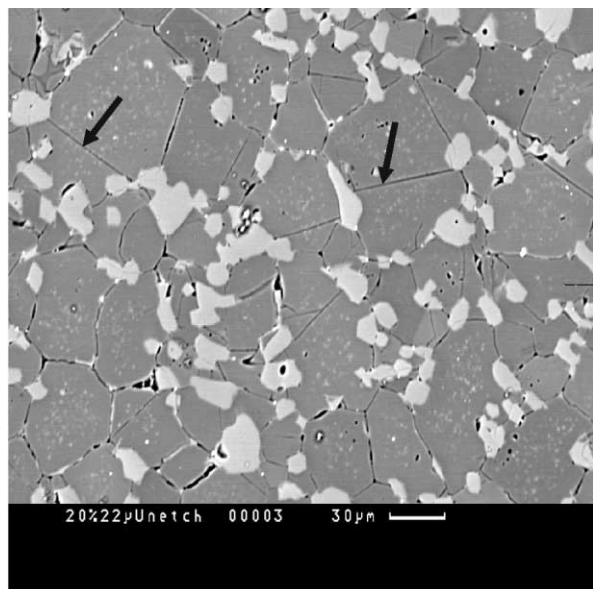


Fig. 4. SEM micrographs of polished surfaces of 20% 22 μm spinel composite materials, showing microcracking (dark gray: MgO, light gray: spinel).

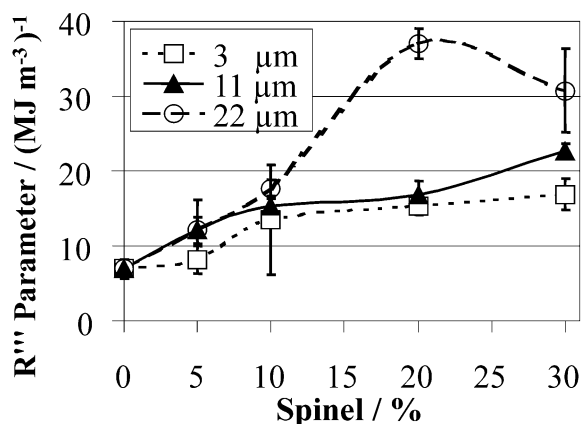


Fig. 5. R''' parameter as a function of spinel content and particle size.

expected that resistance to initiation of fracture caused by thermal stresses would be best with materials containing very high (> 30%) loading of the finest spinel particles (3 μm), and worst for the 22 μm spinel composites. Since the MgO–spinel composites are not very resistant to fracture initiation by the thermal stresses, the R''' and R'''' parameters must be taken into account in characterising further thermal shock damage due to the marked resistance to crack propagation caused by thermal shock.

3.2. R''' parameter

The R''' parameter increased with all spinel additions (Fig. 5). Previous researchers reported that^{22,23} Al_2O_3 had an appreciable solubility in MgO at high temperature, in which the equilibrium mole fraction of Al_2O_3 in MgO is corresponding to ~ 0.02 , at the temperature of

1725 $^\circ\text{C}$ used for preparation of composites. It is considered that the actual spinel content of the composites is approximately 4–5% by weight of Al_2O_3 less than the spinel amounts used because of the solubility of Al_2O_3 in MgO and incomplete re-equilibration on cooling. However, high temperature saturation of the MgO is achieved with increasing additions of spinel (10% and upwards). For this reason, there was probably very little particle size effect, up to 10% spinel additions. The resistance to thermal shock damage of the 3 μm spinel composites would be expected to be similar to that of the 11 μm spinel composites. The strength and Young's modulus values decreased with spinel additions, and the influence of the spinel was observed to be more marked the larger the spinel particle size. Strengths of the coarser spinel composites were in general very much more sensitive to composition than was Young's modulus (Table 1). Composites containing the 22 μm spinel stand out as having significantly higher R''' values, at > 10% loading. The anticipated improvement in thermal shock resistance predicted by the R''' parameter and observed experimentally can be explained by a large decrease in strength, and lesser decrease in modulus (Fig. 1). The large thermal expansion coefficient difference between MgO and spinel, leads to extensive microcracking in composite materials with loss of modulus and strength values.^{24–27} The smaller the spinel particle size, the lesser the concentration of pre-existing connecting cracks due to the thermal expansion mismatch (Figs. 3 and 4). Finer spinel particles (3 and 11 μm) resulted in shorter crack propagation distances from the spinel particle (Fig. 3). However, the 22 μm spinel particles were the origin of longer cracks, and more crack initiation sites (Fig. 4). The micrographs show clearly the tendency for the interlinked networks of cracks to develop, apparently nucleated at the spinel particle surfaces. This tendency is the greater the larger the spinel particle size, and the higher the volume loading. It might therefore have been expected that resistance to crack propagation in general would be greater with materials containing the coarsest spinel particle size.

On the basis of the calculated R''' values, very coarse (> 22 μm median) spinel particles (at > 10% loading) appear to be generally more beneficial than the finer particles, for which a very much larger volume appears to be required to achieve the same improvement. It would here be predicted on this basis that the coarsest (22 μm) spinel would provide a significant improvement (by a factor of > 5) in resistance to thermal shock damage through maximised difficulty of crack propagation, with a maximum at $\sim 20\%$ addition.

3.3. Work of fracture (γ_{WOF})

Values for the measured work of fracture (obtained from the areas under the load–deflection curve) in this

work are comparable to that of 35 J m^{-2} for polycrystalline fully dense MgO (3.56 Mg m^{-3}) of $\sim 100 \mu\text{m}$ average grain size.²⁸ In the composites, there was a general marked increase in γ_{WOF} , by a factor of ~ 2 , up to 30% additions (Fig. 6). The effect of spinel content is much more important than the particle size, within the large scatter band.

Fracture surfaces of pure MgO showed a large proportion of transgranular cracks, with some intergranular cracks (Fig. 7). At low additions of spinel, transgranular cracks were still present with some intergranular cracks, in the fracture surfaces of each spinel composite. However, at higher additions of spinel ($\geq 20\%$), mostly intergranular fracture occurred. The 20% 22 μm spinel composite showed mostly intergranular fracture with some transgranular (Fig. 8). It appears that intergranular cracks in the MgO grains

with increasing spinel additions require much more energy for fracture than MgO (Fig. 6). Spinel composites showed stable crack growth, which indicated significant microcrack extension and bridging (Figs. 3 and 4). Therefore, the higher values of γ_{WOF} are associated with the occurrence of more intergranular fracture (Fig. 8).

3.4. R'''' parameter

The R'''' parameter also increased with spinel additions (Fig. 9). The R'''' parameter for the 11 μm spinel composites showed similar values to the 3 μm spinel composites up to 20% additions, but was more sensitive to particle size with further additions. The 22 μm spinel composites showed the similar trend but there was a larger effect on R'''' above 10% additions, as compared to the other composites. It would be expected that the

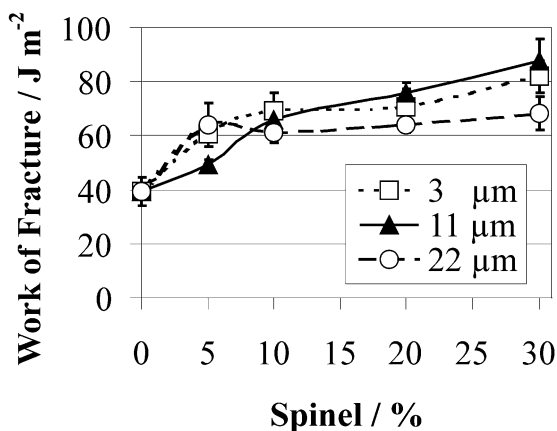


Fig. 6. Work of fracture as a function of spinel content and particle size.

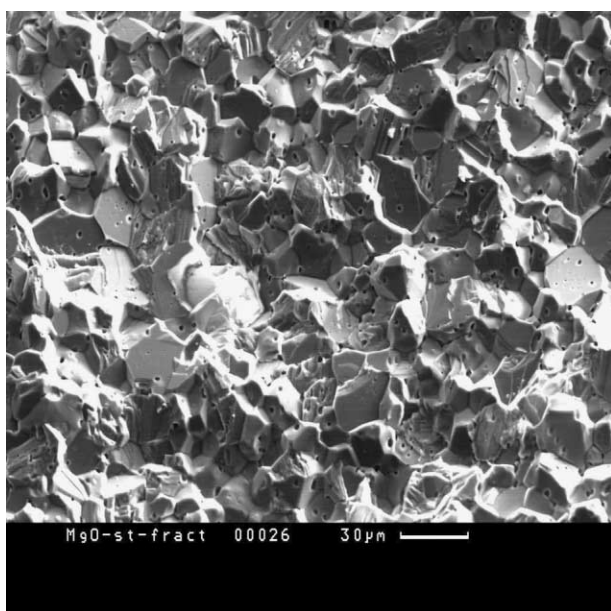


Fig. 7. Fracture surface of dense MgO.

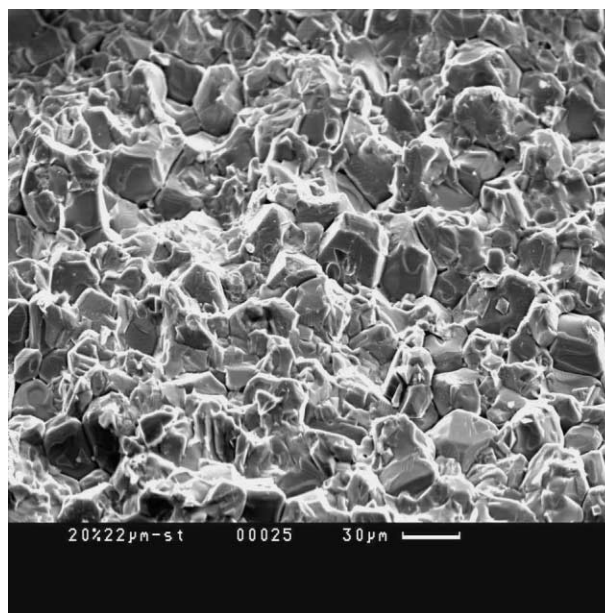


Fig. 8. Fracture surface of composite containing 20% 22 μm spinel.

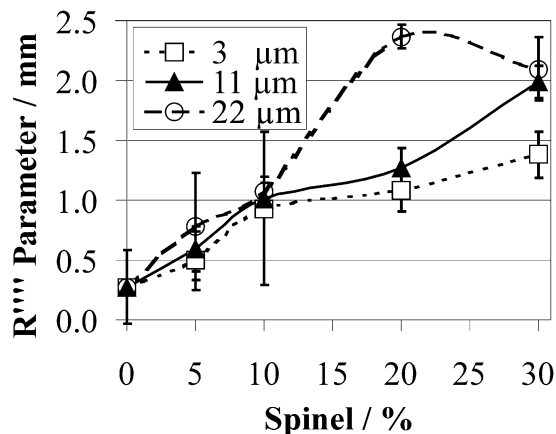


Fig. 9. R'''' parameter as a function of spinel content and particle size.

Table 2
Fraction of initial strengths of MgO and MgO–spinel composites quenched from 1000 °C

ΔT (°C)	Fraction of initial strength			
	MgO (233 MPa ^a)	20% 11 μm (111 MPa ^a)	20% 22 μm (65 MPa ^a)	30% 22 μm (60.5 MPa ^a)
1000	0.23±0.06	0.45±0.09	1.00±0.10	0.89±0.10

^a Initial strength.

20% 22 μm spinel composite would have the highest resistance to thermal shock damage, with an improvement by a factor of ~ 8 , as compared to pure MgO. This increase in R'''' parameter appears mainly to be the result of the marked increase in γ_{WOF} with spinel additions (Fig. 6), and the greater sensitivity of strength to composition and particle size than Young's modulus (Table 1 and Fig. 1).

Basically the R''' and R'''' parameters exhibited similar patterns in terms of variations in spinel content (Figs. 5 and 9). However, the increase in R'''' is more significant, at higher spinel additions, than the increase in R''' , because of the increase in γ_{WOF} (Fig. 6). The amount of extra damage caused by thermal shock is again therefore predicted to be significantly lower with the addition of coarse spinel particles.

For 3 and 11 μm spinel composites, it may be that additions of 30–40% could provide some improvements. Further deterioration of strength in the coarsest spinel composite as a result of thermal shock should be a minimum with 20–30%. In general coarser (22 μm) spinel powders appear to be more beneficial than finer powders, but there is no obvious advantage with additions of $> 30\%$.

3.5. Retained strength after thermal shock

An increase in quench temperature up to 1000 °C resulted in a sharp decrease (77%) in strength for pure MgO (Table 2). In contrast, the spinel composites had a higher retained strength than pure MgO up to the maximum quench temperature used. There was about 55% loss of strength for 20% 11 μm spinel composites, and 11% for 30% 22 μm spinel composites. However, the 20% 22 μm spinel composite did not lose further strength after the quench tests, and in this respect was the most stable of the composites tested. These results showed clearly that the resistance to thermal shock damage for all these materials had the trends expected on the basis of the calculated R''' and R'''' parameters.

4. Conclusions

MgO–spinel composites showed less resistance to fracture initiation by the thermal stresses than MgO

because of the pre-existing cracks caused by thermal expansion mismatch. Finer spinel particles resulted in shorter initial crack propagation distances from the spinel particles; the coarser spinel particles were the origins of longer cracks. It might therefore have been expected that resistance to thermal shock damage, resulting from resistance to microcrack propagation and interlinking, would be higher with materials containing the coarser spinel particle. The occurrence of more intergranular fracture with increasing spinel additions indicated significant microcrack extension and branching, leading to higher γ_{WOF} values.

The R'''' and R''' parameters showed similar patterns in terms of variations with spinel content and particle size, and one was as good as the other. This work confirmed that the R''' and R'''' parameters were good indicators for a quantitative evaluation of the retained strengths. The R''' and R'''' parameters for these model composite materials suggested an optimum composition of 20 to $\sim 30\%$ 22 μm spinel particles. The R''' and R'''' parameters predict that the spinel composites should have greater thermal shock resistance than pure MgO materials (up to 5 to 8 times). Thermal shock results also confirmed that the retained strengths of composite materials after shocking remained much higher (by a factor of 4.5) than those of MgO, and the 20% 22 μm spinel composites are the best at resisting further thermal shock damage and loss of strength.

Acknowledgements

Redland Minerals (UK), and Alcoa International (UK) Ltd. are thanked for supplies of materials. The contributions of Prof. F.L. Riley, who provided suggestions and guidance regarding the direction of the study, and Prof. B. Rand, are gratefully acknowledged. P. Bartha, S. Plint, and M.W. Roberts are thanked for helpful discussions. The contributions of the late Professor R.W. Davidge to the planning of this investigation are acknowledged. Financial support was provided by the Council of Higher Education in Turkey.

References

1. Davidge, R. W. and Tappin, G., Thermal shock and fracture in ceramics. *J. Brit. Ceram. Soc.*, 1967, **66**, 405–422.
2. Hasselman, D. P. H., Elastic energy at fracture and surface energy as design criteria for thermal shock. *J. Am. Ceram. Soc.*, 1963, **46**(11), 535–540.
3. Hasselman, D. P. H. and Singh, J. P., Analysis of thermal stress resistance of microcracked brittle ceramics. *Am. Ceram. Soc. Bull.*, 1979, **58**(9), 856–860.
4. Hasselman, D. P. H., Thermal stress resistance parameters for brittle refractory ceramics: a compendium. *Am. Ceram. Soc. Bull.*, 1970, **49**(12), 1033–1037.

5. Hasselman, D. P. H., Unified theory of thermal shock fracture initiation and crack propagation in brittle ceramics. *J. Am. Ceram. Soc.*, 1969, **52**(11), 600–604.
6. Kingery, W. D., Factors affecting thermal stress resistance of ceramic materials. *J. Am. Ceram. Soc.*, 1955, **38**(1), 3–15.
7. Chaklader, A. C. D. and Bradley, F., Thermal shock resistance parameters and their application to refractories. In *UNITECR '89*, Anaheim, USA, 1989, pp. 1225–1236.
8. Larson, D. R., Coppola, J. A., Hasselman, D. P. H. and Bradt, R. C., Fracture toughness and spalling behaviour of high- Al_2O_3 refractories. *J. Am. Ceram. Soc.*, 1974, **57**(10), 417–421.
9. Sack, R. A., Extension of Griffith's theory of rupture to three dimensions. In *Proc. Physical Soc.*, vol. 58, London, 1946, pp. 729–736.
10. Nakayama, V. and Ishizuka, M., Experimental evidence for thermal shock damage resistance. *Am. Ceram. Soc. Bull.*, 1966, **45**(7), 666–669.
11. Bradt, R. C., Fracture testing of refractories, past present and future. In *Proc. 2nd Int. Conf. on Refractories, Refractories '87*, Vol. 1, Tokyo, 1987, pp. 61–68.
12. Schulle, W., Anh, V. T. and Freiberg, J. U., Improving the thermal shock behaviour of MgO products by selective optimisation of their microstructure. *Veitsch-Radex Rundschau*, 1995, **72**(8), 467–471.
13. Aksel, C., Davidge, R. W., Warren, P. D. and Riley, F. L., Investigation of thermal shock resistance in model magnesia-spinel refractory materials. In *IV. Ceramic Congress*, Proceedings Book, Part 1, Eskişehir, Turkey, 1998, pp. 193–199.
14. Shackelford, J. F., Alexander, W. and Park, J. S., eds., *CRC Materials Science and Engineering Handbook*. CRC Press, Boca Raton, Florida, 1994.
15. Burnett, S. J., *Properties of Refractory Materials*. UKAEA Research Group Report, Harwell, 1969.
16. Soady, J. S., and Plint, S., A quantitative thermal shock approach to the development of magnesia-spinel refractories for the cement kiln. In *UNITECR '91*, Aachen, Germany, 1991, pp. 443–449.
17. British Standard Testing of Engineering Ceramics. BS 7134 Section 1.2, 1989.
18. Standard Test Method for flexural strength of advanced ceramics at ambient temperature. In *Annual Book of ASTM Standards*, Designation: C1161–90, 15.01, 1991, pp. 327–333.
19. Standard Test Methods for flexural properties of unreinforced and reinforced plastics and electrical insulating materials, In *Annual Book of ASTM Standards*, Designation: D790M-86, 08.01, 1988, pp. 290–298.
20. Davidge, R. W. and Tappin, G., The effective surface energy of brittle materials. *J. Mater. Sci.*, 1967, **3**, 165–173.
21. Turner, P. S., Thermal-expansion stresses in reinforced plastics. *J. Res. Natl. Bur. Stand.*, 1946, **37**(4), 239–250.
22. Henriksen, A. F. and Kingery, W. D., The solid solubility of Sc_2O_3 , Al_2O_3 , Cr_2O_3 , SiO_2 and ZrO_2 in MgO. *Ceramurgia Int.*, 1979, **5**(1), 11–17.
23. Hallstedt, B., Thermodynamic assessment of the system MgO- Al_2O_3 . *J. Am. Ceram. Soc.*, 1992, **75**(6), 1497–1507.
24. Aksel, C., Rand, B., Riley, F. L. and Warren, P. D., Mechanical properties of magnesia-spinel composites. *J. Eur. Ceram. Soc.*, 2002, **22**, 745–754.
25. Aksel, C., Davidge, R. W., Warren, P. D. and Riley, F. L., Mechanical properties of model magnesia-spinel composite materials. Euro Ceramics V, Part 3, Extended Abstracts of the 5th Conference and Exhibition of the European Ceramic Society, In *Key Engineering Materials, Vols 132–136*, Versailles, France, 1997, pp. 1774–1777.
26. Aksel, C., Davidge, R. W., Knott, P. and Riley, F. L., Mechanical properties of magnesia-magnesium aluminate spinel composites. In *III. Ceramic Congress Proceedings Book, Vol. 2, Engineering Ceramics*, Istanbul, Turkey, 1996, pp. 172–179.
27. Aksel, C., Thermal shock behaviour and mechanical properties of magnesia-spinel composites. PhD Thesis, Department of Materials Engineering, University of Leeds, Leeds, UK, 1998.
28. Clarke, F. J. P., Tattersall, H. G. and Tappin, G., Toughness of ceramics and their work of fracture. In *Proc. Brit. Ceram. Soc.*, No. 6, 1966, pp. 163–172.